

Observation of Anomalous Momentum Transport in Tokamak Plasmas with No Momentum Input

W. D. Lee, J. E. Rice, E. S. Marmor, M. J. Greenwald, I. H. Hutchinson, and J. A. Snipes

Plasma Science and Fusion Center, MIT, Cambridge, Massachusetts 02139-4307, USA

(Received 9 May 2003; published 13 November 2003)

Anomalous momentum transport has been observed in Alcator C-Mod tokamak plasmas through analysis of the time evolution of core impurity toroidal rotation velocity profiles. Following the L-mode to EDA (enhanced D_α) H-mode transition, the ensuing cocurrent toroidal rotation velocity, which is generated in the absence of any external momentum source, is observed to propagate in from the edge plasma to the core. The steady state toroidal rotation velocity profiles are relatively flat and the momentum transport can be simulated with a simple diffusion model. Velocity profiles during edge localized mode free (ELM-free) H-modes are centrally peaked, which suggests the addition of inward momentum convection. In all operating regimes the observed momentum diffusivities are much larger than the neoclassical values.

DOI: 10.1103/PhysRevLett.91.205003

PACS numbers: 52.55.Fa, 52.30.-q

Rotation and velocity shear play important roles in the transition to high confinement mode (H mode) [1–4], in the formation of internal transport barriers (ITBs) [5] and in suppression of resistive wall modes [6] in tokamak discharges. Compared to energy and particle transport, however, there has been considerably less effort addressing momentum transport. In a majority of tokamak plasmas, the observed toroidal rotation is generated externally by neutral beam injection. By measuring the rotation profiles from the associated beam diagnostics, and calculating the input torque profiles from the beam injection, momentum transport may be characterized [7–14]. Momentum confinement is generally found to be anomalous, with a diffusivity, χ_ϕ , similar to the ion thermal conductivity, χ_i [7–14], but much larger than the neoclassical diffusivity (viscosity). The reliability of this type of analysis depends on the accuracy of the input torque calculations, and the inherent assumption that there is no additional source of momentum when the plasma enters the H mode. Alcator C-Mod ICRF [15] and Ohmic [16] H-mode discharges are found to have substantial spontaneous cocurrent toroidal impurity rotation (as high as 100 km/s, Mach number 0.3) in spite of the fact that there is no momentum input. This calls into question whether the rotation observed in beam heated plasmas is solely externally generated. Similar observations have been made on other devices such as JET [17], COMPASS [18], and Tore Supra [19].

Several attempts to explain the observed rotation in C-Mod have been made, based on ICRF wave driven fast particle orbit shift mechanisms [20,21], turbulence [22,23] and subneoclassical [24] effects. The similarity of the rotation observed in ICRF and purely Ohmic plasmas suggests that it is not due to ICRF wave or fast particle effects. The prediction of reversal of the rotation direction with high magnetic field side off-axis ICRF absorption [20,21] has not been observed in the experiments [25]. For the turbulence driven theories [22,23], the

sign of the rotation is correct, but the magnitude cannot be tested because the turbulence fluctuation levels are not measured. The predictions of the rotation magnitude and direction from the subneoclassical theory agree with the measurements [24], but the calculated momentum diffusion time scale is 2 orders of magnitude longer than what is observed.

In order to gain a better understanding of the mechanism generating the rotation in the absence of an external source, and in general to characterize momentum transport, temporally resolved velocity profiles are needed. Previous off-axis measurements of the Doppler shifts of argon x-ray lines on Alcator C-Mod were along sight lines with only a slight toroidal component [15], so only large rotation velocities could be seen, and only then with poor time resolution. The Alcator C-Mod x-ray crystal spectrometer system has now been modified with three fully tangential views, at $r/a = 0.0, 0.3, \text{ and } 0.6$. These three rotation measurements are augmented by the velocity of magnetic perturbations associated with sawtooth oscillations recorded with an array of fast pickup coils [16]. The time evolution of the observed rotation profiles in H-mode discharges indicates that the source of the momentum is the plasma edge. The momentum propagates to the plasma center on a time scale much faster than expected from the neoclassical diffusivity. In edge localized mode free (ELM-free) H-mode discharges, a large inward momentum pinch is observed. In EDA H-mode plasmas which develop ITBs, the momentum is expelled from inside of the barrier foot.

The rotation observations were obtained from the Alcator C-Mod tokamak, a compact (major radius 0.67 m, minor radius 0.22 m), high magnetic field ($B_T \leq 8$ T) device with strong shaping capabilities and all metal plasma facing components. Auxiliary heating is available with up to 4 MW of ICRF heating power at 80 MHz. For the plasmas described here, the hydrogen minority heating was with $0 - \pi$ phasing, and there was no momentum

input. Shown in Fig. 1 are the time histories of the (impurity) toroidal rotation velocities at three radii and the rotation of magnetic perturbations in precursors and postcursors of sawtooth oscillations, for a 2.0 MW ICRF heated EDA H-mode [26] plasma. This 0.8 MA, 5.3 T discharge entered EDA H mode at 0.655 s, as indicated by the drop in the D_α signal, with a subsequent increase in the plasma stored energy and toroidal rotation velocity [15]. The velocity increase was first seen on the outermost spectrometer ($r/a = 0.6$), sequentially moving inside, suggesting an edge source of toroidal momentum which propagated in towards the center, with a time scale somewhat longer than τ_E , the energy confinement time. After about 150 ms (0.8 s), the rotation settled to a value of ~ 50 km/s (in the cocurrent direction), with a flat profile. During this steady phase of the discharge, the central electron density was $2.8 \times 10^{20}/\text{m}^3$ and the central electron temperature was 2.1 keV. Similar velocity profile evolution has been seen in purely Ohmic EDA H-mode plasmas without ICRF heating. This time evolution and flat steady state rotation profile suggest that the momentum transport in EDA H-mode plasmas may be characterized by a purely diffusive process. The situation is different in ELM-free H-mode plasmas, as can be seen in Fig. 2. This 0.8 MA, 4.6 T discharge entered the ELM-free H mode at 0.624 s, reverted to the L mode at 0.834 s, then reentered the ELM-free H mode at 0.871 s. Following both L-H transitions, there was a rapid increase in the

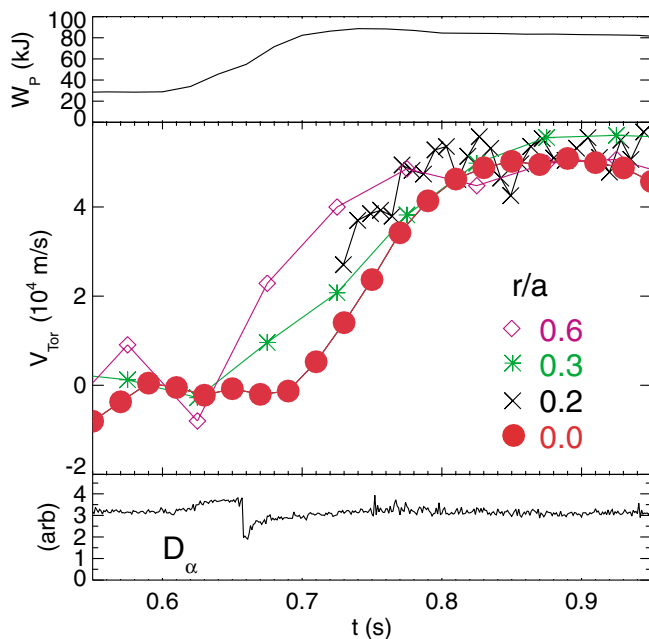


FIG. 1 (color). The plasma stored energy, impurity toroidal rotation velocity at three radii (red dots, green asterisks, and purple diamonds for $r/a = 0.0, 0.3,$ and $0.6,$ respectively), magnetic perturbation rotation (\times) at the sawtooth inversion radius ($r/a \sim 0.2$), and the edge D_α brightness for an ICRF heated EDA H-mode discharge.

core rotation velocity and stored energy. In contrast to the EDA H-mode case, these rotation profiles are highly peaked [15], reaching ~ 70 km/s in the core and ~ 15 km/s at $r/a = 0.6$. This demonstrates momentum transport up the velocity gradient and suggests the presence of an inward momentum pinch [12]. During the first ELM-free period, the central electron temperature was relatively constant at 1750 eV, while the electron density rose continuously from 1.1×10^{20} to $2.9 \times 10^{20}/\text{m}^3$, maintaining a flat profile. In contrast to these peaked rotation profiles are the hollow profiles which develop in ITB plasmas. ITB discharges can be produced with off-axis ICRF heating [25,27], provided the resonance location is outside of $r/a = 0.5$ and that the plasma first enters the EDA H mode. These ITBs are characterized by a strong peaking of the core electron density which evolves in conjunction with a decrease and reversal of the core toroidal rotation velocity [25,27]. Shown in Fig. 3 are the rotation time histories for a 4.5 T, 0.8 MA EDA H-mode plasma produced with 2.2 MW of off-axis ICRF heating power at 80 MHz. Up until 0.85 s, this plasma exhibited the normal EDA H-mode rotation characteristics (Fig. 1) with the velocity propagating in from the outside, and the profile becoming flat across most of the plasma. After 0.85 s, the core rotation inside $r/a = 0.5$ (the location of the barrier foot) dropped and reversed direction simultaneously with a strong peaking of the electron density profile also inside of $r/a = 0.5$. The rotation at $r/a = 0.6,$

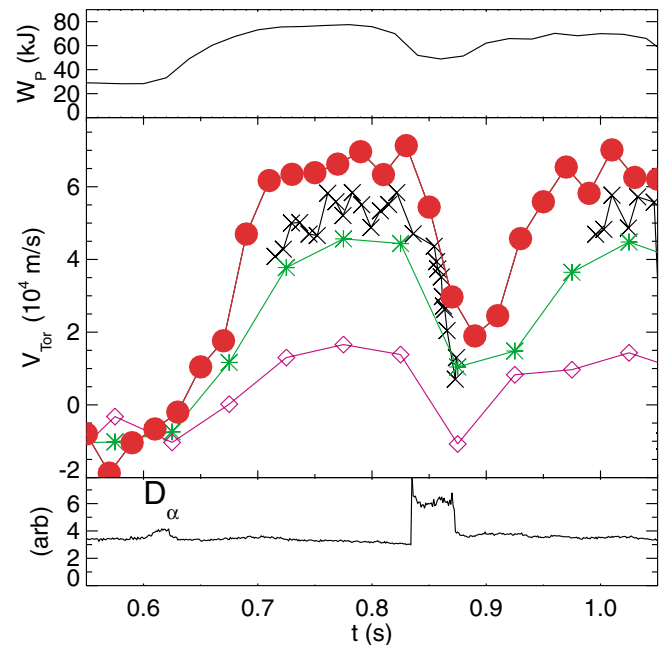


FIG. 2 (color). The plasma stored energy, impurity toroidal rotation velocity at three radii (red dots, green asterisks, and purple diamonds for $r/a = 0.0, 0.3,$ and $0.6,$ respectively), magnetic perturbation rotation (\times) at the sawtooth inversion radius ($r/a \sim 0.2$), and the edge D_α brightness for an ICRF heated ELM-free H-mode discharge.

outside of the barrier foot, decreased more slowly and not so far, indicating a positive velocity gradient in the vicinity of the ITB foot. The radial electric field, E_r , determined from the force balance equation and from calculations of the poloidal magnetic field, assuming neoclassical poloidal velocity, was found to be -10 kV/m at $r/a = 0.3$ (inside of the ITB foot) and $+5$ kV/m at $r/a = 0.6$ (outside of the foot), and a lower limit of the E_r gradient is ~ 250 kV/m² at 1.1 s.

The evolution of the velocity profiles has been simulated using a simple source-free momentum transport model

$$\frac{\partial}{\partial t}P + \nabla \cdot \left(-D_\phi \frac{\partial}{\partial r}P - \frac{v_c r}{a}P \right) = 0 \quad (1)$$

with $P = n_i m_i V_\phi$, where a is the minor radius and where the momentum diffusivity, D_ϕ , and the momentum convection velocity, v_c , are free parameters to be determined. In cylindrical coordinates and subject to the boundary conditions of an edge rotation, V_0 , during the H mode

$$V_\phi(a, t) = \begin{cases} 0, & t < t_{L \rightarrow H} \\ V_0, & t_{L \rightarrow H} \leq t \leq t_{H \rightarrow L} \\ 0, & t > t_{H \rightarrow L} \end{cases} \quad (2)$$

and with the assumptions (observed in the electrons) of a flat ion density profile, and spatially and temporally constant D_ϕ and v_c , the toroidal rotation velocity, V_ϕ , profile evolution may be determined from a solution to

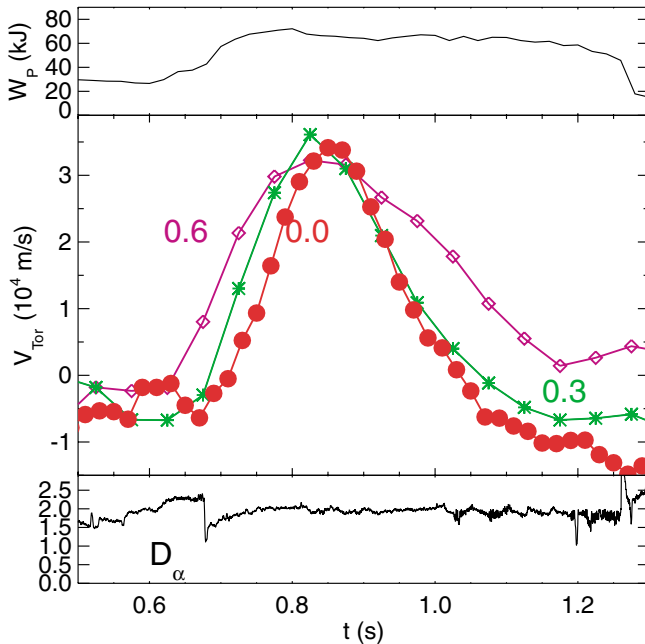


FIG. 3 (color). The plasma stored energy, impurity toroidal rotation velocity at three radii, and the edge D_α brightness for an off-axis ICRF heated ITB discharge.

$$\frac{\partial}{\partial t}V_\phi - D_\phi \left[\frac{\partial^2}{\partial r^2}V_\phi + \left(\frac{1}{r} + \frac{v_c r}{aD_\phi} \right) \frac{\partial}{\partial r}V_\phi + \frac{2v_c}{aD_\phi}V_\phi \right] = 0 \quad (3)$$

via an expansion in confluent hypergeometric functions.

An example of a comparison of this model to the observed velocity time evolution in an EDA H-mode plasma similar to that presented in Fig. 1 is shown in the top frame of Fig. 4. The time of the L- to H-mode transition was 1.11 s. The three curves represent the simulated rotation velocities at the radii of the three spectrometer views. For this case, D_ϕ was spatially constant with a value of 0.05 m²/s, and $v_c \approx 0$, which corresponds to a momentum confinement time, τ_ϕ , of 150 ms. This momentum diffusivity is much greater than the neoclassical viscosity, $\chi_\phi \sim \rho_i^2/\tau_{ii} \sim 0.003$ m²/s for this case, and the momentum transport may be characterized as anomalous. The momentum diffusivity may also be determined for the L mode from the decay of the rotation velocity after the H- to L-mode transition at 1.53 s; D_ϕ for the L-mode portion of this discharge was 0.20 m²/s, with $\tau_\phi \sim 35$ ms. From modeling of several ICRF and Ohmic EDA H-mode plasmas, D_ϕ was found to be in the range from 0.05 to 0.10 m²/s, with $v_c \approx 0$. The simulations for the ELM-free discharge from Fig. 2 are shown in the bottom frame of Fig. 4, which is on the same time scale as the top frame for comparison. In this instance D_ϕ was 0.40 m²/s with $v_c = 12$ m/s, and $\tau_\phi \sim 70$ ms. This value of the pinch velocity was necessary to match the quasisteady peaked profile shape at 0.8 s, with a

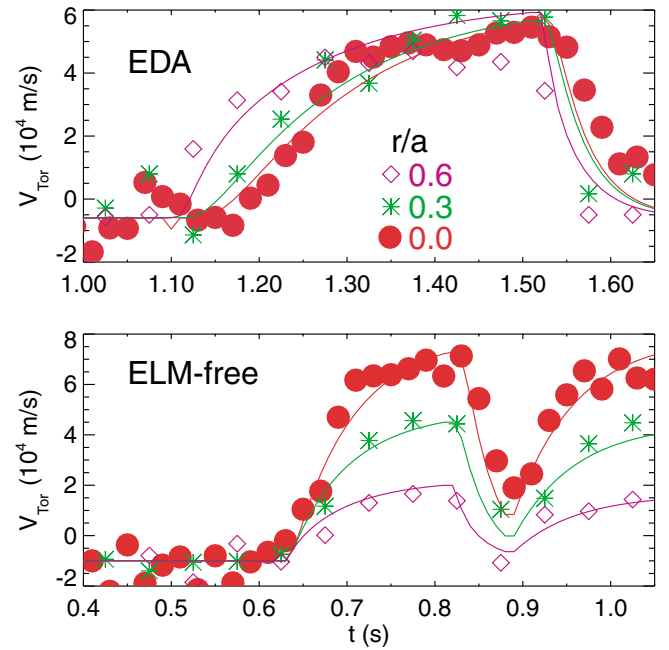


FIG. 4 (color). Comparison of model calculations (solid lines) with observed rotation time histories for an EDA H-mode plasma (top frame) and an ELM-free H-mode plasma (bottom frame).

“peaking factor,” $S \equiv av_c/2D_\phi = 3.2$, along with the overall rise time of the rotation, with $v_c = 0$.

The model of Eq. (3) cannot be strictly applied to the ITB case in Fig. 3 because the electron (ion) and argon density profiles [27] were peaking in the core during the barrier evolution. However, along with the negative rotation velocity inside of the barrier foot, this implies a negative momentum density in the core, which would require an outward momentum convection in the core during the ITB phase.

In the progression from the L mode to the EDA H mode to the ELM-free H mode to ITB discharges, the particle diffusivity steadily drops (particle confinement increases), approaching neoclassical levels in the core in ITB plasmas. EDA H-mode plasmas have temporally and spatially constant electron density profiles, ELM-free H-mode plasmas exhibit steadily rising electron density profiles which maintain a flat shape, and ITB discharges show a central peaking of the density profile [25,27] consistent with the neoclassical Ware pinch velocity. The same sequence of impurity confinement may be characterized as highly anomalous in the L mode, with an impurity diffusivity $D_I \sim 0.5 \text{ m}^2/\text{s}$ ($\tau_I \sim 15\text{--}25 \text{ ms}$) and $D_I \sim 0.1\text{--}0.3 \text{ m}^2/\text{s}$ in the EDA H mode with $\tau_I \sim 50\text{--}150 \text{ ms}$ [28]. For ELM-free H-mode plasmas, the impurity confinement is long ($\tau_I \sim 1 \text{ s}$) with reduced D_I ($\sim 0.05 \text{ m}^2/\text{s}$) and substantial inward convection ($10\text{--}100 \text{ m/s}$) at the edge [28]. In ITB discharges there is strong core impurity accumulation [27] with D_I ($\sim 0.02 \text{ m}^2/\text{s}$) and v_I ($\sim 100 \text{ ms}$ inward) close to the neoclassical values in the core plasma. Energy confinement exhibits a somewhat similar progression with χ_{eff} dropping from $\sim 1 \text{ m}^2/\text{s}$ in the L mode to $\sim 0.5 \text{ m}^2/\text{s}$ in the H mode [26] and then as far as $\sim 0.1 \text{ m}^2/\text{s}$ (near the neoclassical level) in the core plasma during ITB [27] operation. Momentum confinement demonstrates some similarities in behavior; there is a decrease in the momentum diffusivity from $0.20\text{--}0.25 \text{ m}^2/\text{s}$ in the L mode to the range $0.05\text{--}0.10 \text{ m}^2/\text{s}$ in the EDA H mode. Also, in the ELM-free H mode there is a strong momentum pinch, with $v_c \sim 10 \text{ m/s}$, analogous to the observations of impurity transport. In ITB discharges, particle, impurity, and energy confinement may be characterized by transport coefficients with values similar to neoclassical levels in the core. For these discharges, however, the momentum seems to be expelled from the plasma center, rather than having increased confinement. The reason that the momentum transport in ITB discharges does not follow the behavior of particle and energy confinement may be because these plasmas have a negative E_r well in the core and may be influenced by the fact that momentum is an odd moment of the distribution function, having directionality.

Following the H-mode transition in Alcator C-Mod discharges, toroidal momentum is observed to propagate

in from the plasma edge, although there is no external source. The momentum transport has been found to be anomalous, with momentum diffusivities much larger than neoclassical levels. In ELM-free plasmas, there is evidence for an inward momentum pinch, while in ITB discharges, the momentum is expelled from the core. The cause of the toroidal rotation, generated in the absence of a momentum source, as well as the varying velocity profile shapes, remains unexplained.

The authors thank A. Hubbard for T_e measurements, S. Wolfe for magnetic equilibrium calculations, J. Terry for D_α measurements, P. Bonoli and S. Scott for useful discussions, S. Wukitch and Y. Lin for operation of the ICRF systems, and J. Irby and the Alcator C-Mod operations group for expert running of the tokamak. This work was supported at MIT by DoE Contract No. DE-FC02-99ER54512.

-
- [1] K. C. Shaing and E. C. Crume, Phys. Rev. Lett. **63**, 2369 (1989).
 - [2] H. Biglari *et al.*, Phys. Fluids B **2**, 1 (1990).
 - [3] R.J. Groebner *et al.*, Phys. Rev. Lett. **64**, 3015 (1990).
 - [4] K. Ida *et al.*, Phys. Rev. Lett. **65**, 1364 (1990).
 - [5] K. Burrell, Phys. Plasmas **4**, 1499 (1997).
 - [6] E. J. Strait *et al.*, Phys. Rev. Lett. **74**, 2483 (1994).
 - [7] S. Suckewer *et al.*, Nucl. Fusion **21**, 1301 (1981).
 - [8] K. H. Burrell *et al.*, Nucl. Fusion **28**, 3 (1988).
 - [9] S. D. Scott *et al.*, Phys. Rev. Lett. **64**, 531 (1990).
 - [10] A. Kallenbach *et al.*, Plasma Phys. Controlled Fusion **33**, 595 (1991).
 - [11] N. Asakura *et al.*, Nucl. Fusion **33**, 1165 (1993).
 - [12] K. Nagashima *et al.*, Nucl. Fusion **34**, 449 (1994).
 - [13] K.-D. Zastrow *et al.*, Nucl. Fusion **38**, 257 (1998).
 - [14] J. S. deGrassie *et al.*, Nucl. Fusion **43**, 142 (2003).
 - [15] J. E. Rice *et al.*, Nucl. Fusion **38**, 75 (1998).
 - [16] I. H. Hutchinson *et al.*, Phys. Rev. Lett. **84**, 3330 (2000).
 - [17] L.-G. Eriksson *et al.*, Plasma Phys. Controlled Fusion **39**, 27 (1997).
 - [18] I. H. Coffey *et al.*, in *Proceedings of the 11th Colloquium on UV and X-Ray Spectroscopy of Astrophysical and Laboratory Plasmas, Nagoya, Japan, 1995*, Frontiers Science Series No. 15, edited by K. Yamashita and T. Watanabe (Universal Academy Press, Tokyo, Japan, 1996), p. 431.
 - [19] G. T. Hoang *et al.*, Nucl. Fusion **40**, 913 (1999).
 - [20] F. W. Perkins *et al.*, Phys. Plasmas **8**, 2181 (2001).
 - [21] L.-G. Eriksson and F. Porcelli, Nucl. Fusion **42**, 959 (2002).
 - [22] K. C. Shaing, Phys. Rev. Lett. **86**, 640 (2001).
 - [23] B. Coppi, Nucl. Fusion **42**, 1 (2002).
 - [24] A. L. Rogister *et al.*, Nucl. Fusion **42**, 1144 (2002).
 - [25] J. E. Rice *et al.*, Nucl. Fusion **41**, 277 (2001).
 - [26] M. Greenwald *et al.*, Nucl. Fusion **37**, 793 (1997).
 - [27] J. E. Rice *et al.*, Nucl. Fusion **42**, 510 (2002).
 - [28] J. E. Rice *et al.*, Phys. Plasmas **4**, 1605 (1997).